



Low-temperature heat capacity of triangle antiferromagnetic molecular clusters $K_{12}[(VO)_3(SbW_9O_{33})_2] \cdot 15H_2O$ and $K_{12}[(VO)_3(BiW_9O_{33})_2] \cdot 29H_2O$

Yoshimitsu Kohama^{a,*}, Hitoshi Kawaji^a, Tooru Atake^a, Keisuke Fukaya^b, Toshihiro Yamase^b

^a Materials and Structures Laboratory, Tokyo Institute of Technology, R3-7, 4259 Nagatsuta-cho, Midori-ku, Yokohama 226-8503, Japan

^b Chemical Resources Laboratory, Tokyo Institute of Technology, R1-21, 4259 Nagatsuta-cho, Midori-ku, Yokohama 226-8503, Japan

ARTICLE INFO

Article history:

Received 25 September 2008

Accepted 26 March 2009

Available online 5 April 2009

PACS:

75.50.Xx

75.40.Cx

Keywords:

Molecular magnets

Heat capacity

Energy level diagram

ABSTRACT

Energy level diagrams have been determined for two molecular clusters, $K_{12}[(VO)_3(SbW_9O_{33})_2] \cdot 15H_2O$ and $K_{12}[(VO)_3(BiW_9O_{33})_2] \cdot 29H_2O$, by low-temperature heat capacity measurements down to 85 mK under magnetic field strengths up to 9 T. Both compounds exhibit a broad heat capacity peak dependent upon the magnetic field, which can be explained by the thermal excitation in the magnetic energy levels. A detailed analysis based on the numerical calculation reveals that the spin–spin interaction between the V^{4+} ions includes a Dzyaloshinskii–Moriya interaction.

© 2009 Elsevier Inc. All rights reserved.

1. Introduction

In recent years, magnetic molecular clusters have been attracting broad interest because of their technological [1–3] and scientific importance [4]. These molecular clusters are composed of various magnetic atoms (for instance, Cu, Cr, Fe, and V), in which the spin correlation between these atoms is a major factor affecting the magnetic energy structure. One important issue in this field is how the magnetic energy structure depends upon the molecular structure, the spin number, and the magnetic interactions. In particular, the study of energy structure in the quantum spin system ($S = 1/2$) with triangular structure has been extensively studied in order to understand the strong quantum fluctuation and the geometrical frustration effect [5,6]. However, the research has been mostly investigated by magnetic and optical measurements [6,7], and calorimetric studies are still lacking.

Recently, we reported a vanadium-based triangular molecular cluster, $[(VO)_3(XW_9O_{33})_2]^{12-}$ ($X = Sb^{3+}$ and Bi^{3+}) [8–10]. Three magnetic vanadium ions (V^{4+} ; $S = 1/2$) construct the triangular structure $[(VO)_3]^{6+}$, and the vanadium ion triangle is sandwiched between two diamagnetic α - β - $[XW_9O_{33}]^{9-}$ ligands. The distance between the V^{4+} ions is 5.32–5.36 Å in the $[(VO)_3(SbW_9O_{33})_2]^{12-}$ anion [10] and 5.38–5.48 Å in the $[(VO)_3(BiW_9O_{33})_2]^{12-}$ anion [8,9]. Therefore, the $[(VO)_3]^{6+}$ triangular clusters can be described

as a slightly distorted equilateral triangle [8–10]. The three spins of V^{4+} ions should lead to an energy structure consisting of eight states that are two Kramer's doublets ($S^T = 1/2$) with different spin chirality and a quartet excited level ($S^T = 3/2$). In an earlier paper, Yamase et al. suggested that, as a result of magnetic and optical measurements, the two Kramer's doublets degenerate in $K_{12}[(VO)_3(SbW_9O_{33})_2] \cdot 27H_2O$ [8]. However, they also pointed out the presence of the Dzyaloshinskii–Moriya (DM) antisymmetric exchange interaction and the slightly distorted triangle structure [12], which should induce the separation of those doublets [11,12]. To resolve the discrepancy, a precise investigation of the low-lying energy levels is needed.

In this study, we report the results of the heat capacity measurements on two molecular clusters, $K_{12}[(VO)_3(SbW_9O_{33})_2] \cdot 15H_2O$ and $K_{12}[(VO)_3(BiW_9O_{33})_2] \cdot 29H_2O$, and demonstrate the separation of those Kramer's doublets. Unlike the magnetization and ESR measurements, heat capacity measurements can estimate the energy structure without applying magnetic fields. Therefore, this method avoids the detrimental effects of the energy-level broadening under magnetic fields, and makes it possible to determine the precise energy level at zero field.

2. Experimental

The samples were prepared as described previously [9]. The crystals were $K_{12}[(VO)_3(SbW_9O_{33})_2] \cdot 15H_2O$ (denoted by $(VO)_3Sb$)

* Corresponding author. Fax: +1 505 665 4311.

E-mail address: ykohama@lanl.gov (Y. Kohama).

[10] and $K_{12}[(VO)_3(BiW_9O_{33})_2] \cdot 29H_2O$ (denoted by $(VO)_3Bi$ [8,9]. Although a slight deviation of the composition from the previously synthesized compound [8,9] was observed in $(VO)_3Sb$, the composition of the anionic part $[(VO)_3(SbW_9O_{33})_2]^{12-}$ forming the triangle was not changed [9,10]. The heat capacity of both samples was measured by a homemade relaxation-type calorimeter using a $^3He/^4He$ dilution refrigerator between 85 mK and 5 K under magnetic fields up to 9 T [13]. The weights of the samples used for heat capacity measurements were 2.520 and 1.965 mg for $(VO)_3Sb$ and $(VO)_3Bi$, respectively.

3. Results and discussion

Figs. 1 and 2 show the molar heat capacity C_p of $(VO)_3Sb$ and $(VO)_3Bi$, respectively, under a range of magnetic fields. Both compounds exhibit a broad peak at around 2 K under zero magnetic field, and the shape of the peak varies with changes in the magnetic field. The change of shape indicates that the energy levels in this spin system are split under magnetic fields as a result of the Zeeman effect. To estimate the contribution of the spin system, we express the C_p as

$$C_p = C_{lat} + C_{Sch}, \quad (1)$$

where C_{lat} is the lattice contribution and C_{Sch} is the Schottky heat-capacity due to the thermal excitation of the spin system. At low temperatures, the C_{lat} can be given by

$$C_{lat} = aT^3 + bT^5, \quad (2)$$

and C_{Sch} of the system is written as

$$C_{Sch} = T \frac{d^2(RT \ln z)}{dT^2}, \quad (3)$$

where R is the gas constant and z is the partition function. The quantity z is defined by

$$z = \sum_{i=1}^8 \exp\left(\frac{-E_i}{k_B T}\right). \quad (4)$$

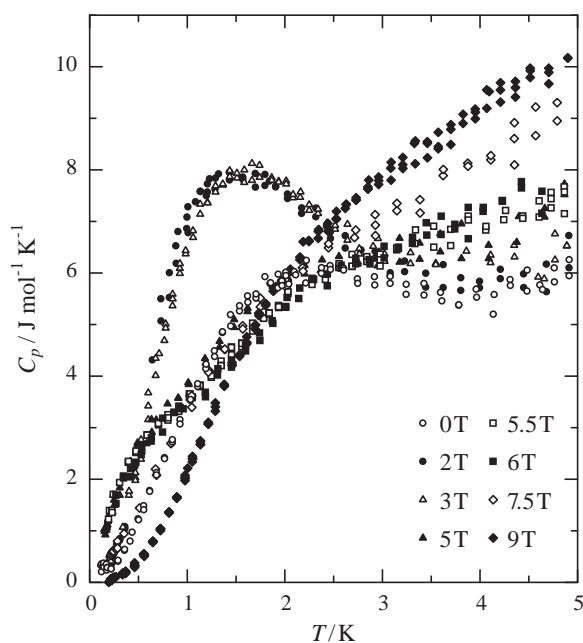


Fig. 1. Low-temperature heat capacity of $K_{12}[(VO)_3(SbW_9O_{33})_2] \cdot 15H_2O$ under various magnetic fields.

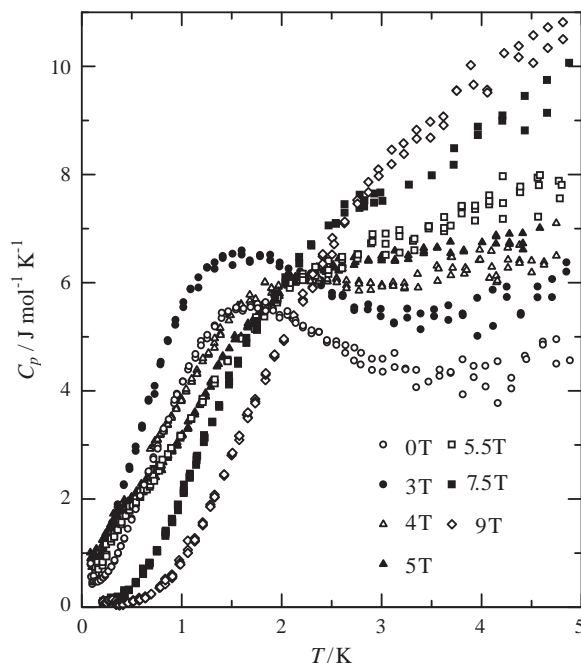


Fig. 2. Low-temperature heat capacity of $K_{12}[(VO)_3(BiW_9O_{33})_2] \cdot 29H_2O$ under various magnetic fields.

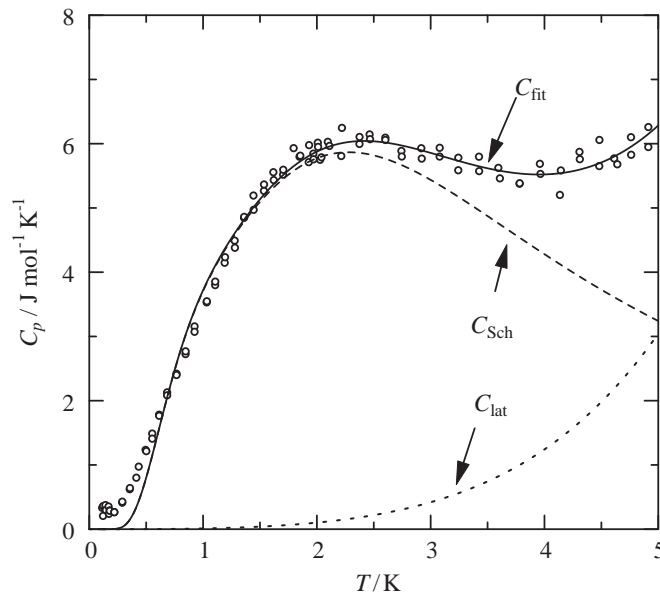


Fig. 3. C_p vs T under zero magnetic field of $K_{12}[(VO)_3(SbW_9O_{33})_2] \cdot 15H_2O$. The solid curve is our best fit using Schottky analysis, the dotted curve is the lattice contribution, and the dashed curve is the Schottky contribution (see the text).

where k_B is the Boltzmann constant, and E_i is the energy of the i th state. As mentioned previously, the eight energy states consist of two Kramer's doublets ($S^T = 1/2$) and a quartet ($S^T = 3/2$) under zero magnetic field [11,12]. To express the energy structure under zero magnetic field, we used two fitting parameters, δ_1 and δ_2 . δ_1 represents the energy difference between two doublets, and the δ_2 represents the energy difference between the ground state doublet and the quartet. Fig. 3 shows the calculated curve (C_{fit}) with the four fitting parameters ($a = 10.6 \text{ mJ mol}^{-1} \text{ K}^{-4}$, $b = 0.55 \text{ mJ mol}^{-1} \text{ K}^{-6}$, $\delta_1 = 2.9 \text{ K}$ and $\delta_2 = 8.2 \text{ K}$), which is well fitted to C_p . The value of δ_1 is not in agreement with the value reported earlier ($\delta_1^{MST} = 0.0 \text{ K}$, $\delta_2^{MST} = 7.2 \text{ K}$) in $K_{11}H[(VO)_3(SbW_9O_{33})_2] \cdot 27H_2O$ that was estimated by magnetization step

(MST) measurements [8]. The disagreement may be caused by the rough estimation of δ_1 by previous MST measurements. To estimate δ_1^{MST} , the observation of the magnetization step corresponding to the energy-level crossing between the first excited state ($S^T = 1/2$) and the second excited state ($S^T = 3/2$) is required. However, the signal of the magnetization step should be significantly weak in the crossing between excited states, because the magnitude of the signals is proportional to the population of the energy level at the measurement temperature. In addition, the DM interaction and the use of powder samples should lead to the broadening of the magnetization step in the previous MST measurements [8,14]. Therefore, the present estimate of δ_1 by heat capacity measurement seem to be appropriate for $(\text{VO})_3\text{Sb}$.

We also tried to estimate the C_p of $(\text{VO})_3\text{Bi}$ under zero magnetic field in the same manner. In the previous MST measurements [8], the saturated magnetization of $(\text{VO})_3\text{Bi}$ is only $\sim 85\%$ of the theoretical value, suggesting that the sample of $(\text{VO})_3\text{Bi}$ deviates from the nominal composition. Therefore, in this study we added one adjustable parameter (c) as follows:

$$C_p = C \times (C_{\text{Sch}} + C_{\text{lat}}) \quad (5)$$

Then, the calculated curve (C_{fit}^*) can be fitted well to the C_p with the parameters ($a = 22.9 \text{ mJ mol}^{-1} \text{ K}^{-4}$, $b = 0.227 \text{ mJ mol}^{-1} \text{ K}^{-6}$, $\delta_1 = 2.3 \text{ K}$, $\delta_2 = 6.2 \text{ K}$ and $c = 0.90$) (Fig. 4). The value of c is in good agreement with the ratio of the observed magnetization value to the theoretical saturation value in the previous MST measurements, indicating that the number of the spin systems is actually less than that for the nominal composition of the $(\text{VO})_3\text{Bi}$ sample. δ_2 also agrees with the previous MST measurements, but δ_1 is not in good agreement with the previous MST measurements ($\delta_1^{\text{MST}} = 1.4 \text{ K}$, $\delta_2^{\text{MST}} = 6.6 \text{ K}$) [8]. The discrepancy might be caused by the difficulty of estimating δ_1 using measurement of MST.

In order to analyze the degeneracy of the energy levels under various magnetic fields, we calculated the entropy of the spin system (ΔS) from the excess heat capacity (ΔC_p) under various magnetic fields for $(\text{VO})_3\text{Sb}$ (Fig. 5) and $(\text{VO})_3\text{Bi}$ (Fig. 6). Here, ΔC_p corresponds to the Schottky contribution (C_{Sch}) that is calculated by subtraction of the lattice contributions from the total heat capacity, given by $C_p - C_{\text{lat}}$ for $(\text{VO})_3\text{Sb}$ and $C_p/c - C_{\text{lat}}$ for $(\text{VO})_3\text{Bi}$. Both compounds show similar entropy curves, indicating a similar

energy structure. Under zero magnetic field, the ΔS of $(\text{VO})_3\text{Sb}$ and $(\text{VO})_3\text{Bi}$ shows a tendency to saturate at $R \ln 4$. This value clearly shows that the degeneracy between the two Kramers's doublets

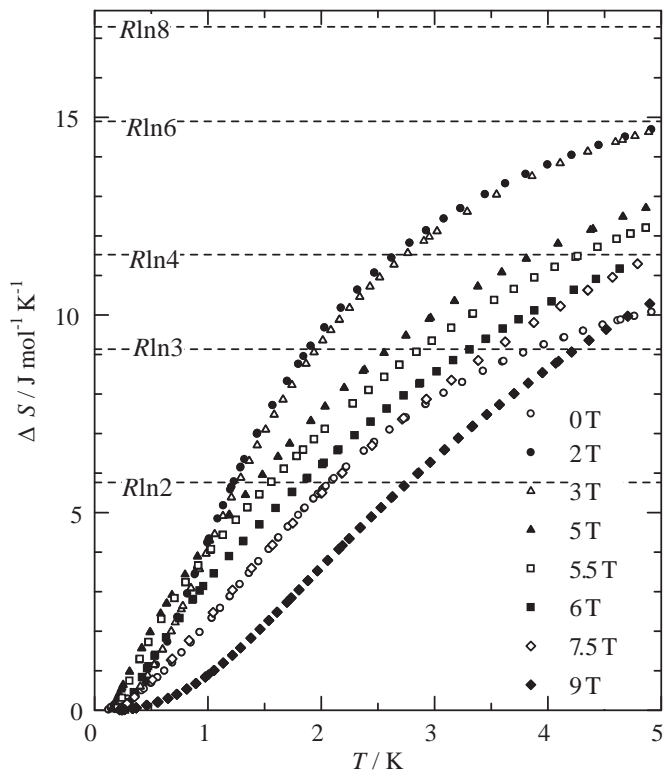


Fig. 5. Temperature dependence of the magnetic entropy in $\text{K}_{12}[(\text{VO})_3(\text{Sb}-\text{W}_9\text{O}_{33})_2] \cdot 15\text{H}_2\text{O}$.

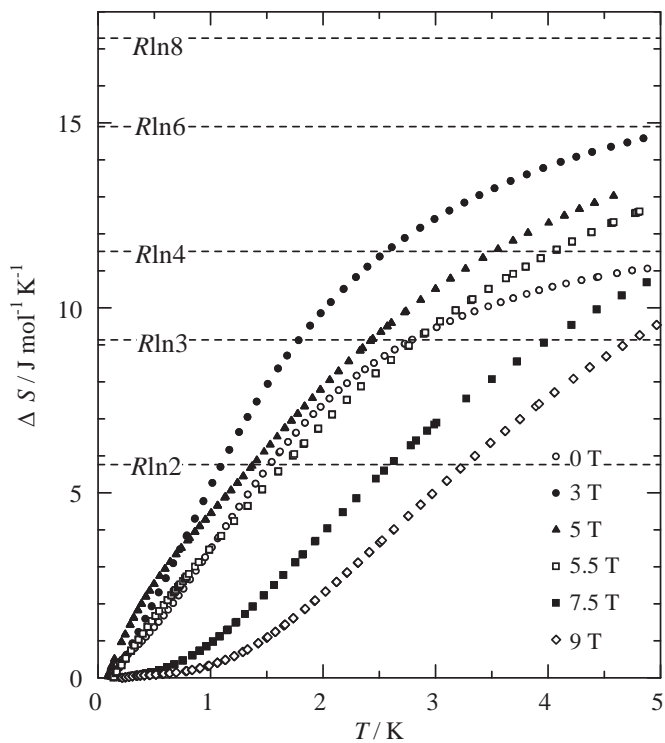


Fig. 6. Temperature dependence of the magnetic entropy in $\text{K}_{12}[(\text{VO})_3(\text{Bi}-\text{W}_9\text{O}_{33})_2] \cdot 29\text{H}_2\text{O}$.

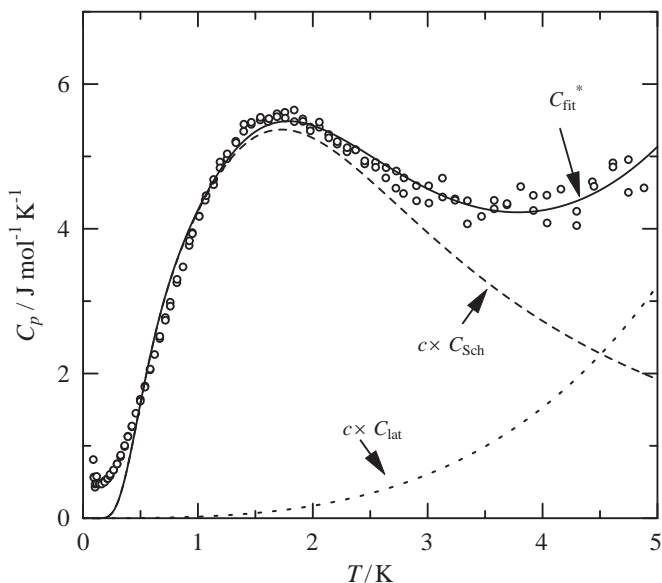


Fig. 4. C_p vs T under zero magnetic field of $\text{K}_{12}[(\text{VO})_3(\text{BiW}_9\text{O}_{33})_2] \cdot 29\text{H}_2\text{O}$. The solid curve is the best-fit curve, the dotted curve is the lattice contribution, and the dashed curve is the calculated Schottky contribution (see the text).

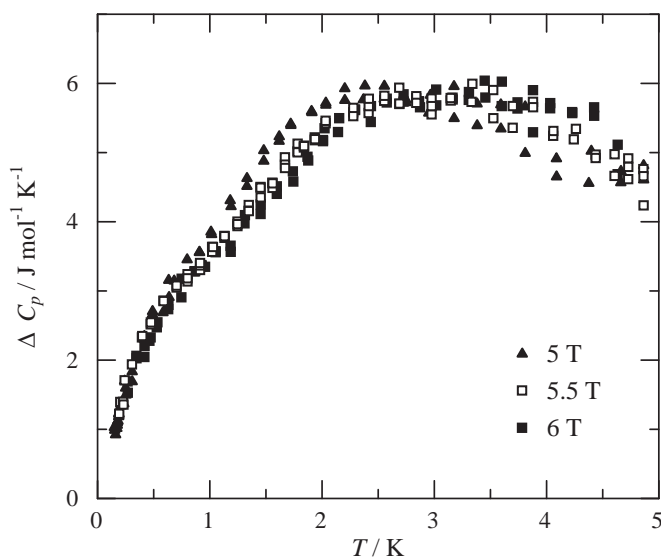


Fig. 7. ΔC_p vs T plot in $K_{12}[(VO)_3(SbW_9O_{33})_2] \cdot 15H_2O$ between 5 and 6 T.

in $(VO)_3Sb$ and $(VO)_3Bi$ is lifted under zero magnetic field by the DM interaction, the distortion, and other factors. Under magnetic fields, the ΔS clearly exceeds $R \ln 4$ up to 3 T, and further increase of the magnetic field leads to a decrease of ΔS . The decrease of ΔS might indicate that the Zeeman splitting becomes too large to reach saturation in the temperature range of these measurements. Thus, the saturation value of ΔS under magnetic fields is essentially larger than $R \ln 4$. The high saturation value under magnetic fields also supports that the ground state consists of a Kramers's doublet under a zero magnetic field.

Previous MST measurements [8] suggest that the energy level crossing between the ground state ($S^T = 1/2$) and the first excited state ($S^T = 3/2$) occurs near 5.5 T in $K_{11}H[(VO)_3(SbW_9O_{33})_2] \cdot 27H_2O$. To investigate that proposal in detail near the energy level crossing field, the ΔC_p under 5, 5.5, and 6 T are plotted in Fig. 7. Below 1 K, ΔC_p is almost independent of the magnetic field, while above 1 K, ΔC_p depends somewhat on the magnetic field, reflecting the Zeeman splitting. This indicates that, near the energy level crossing field, the energy gap between the ground state and the first excited state is hardly changed by the magnetic field. Such phenomena cannot be explained by Zeeman splitting alone and are apparently caused by the energy-level repulsions, which are produced by some interactions, such as DM interaction, hyperfine interaction, and so forth [12,14]. The DM interaction is the most likely candidate for such energy-level repulsion [6,12,14], and, in fact, the earlier MST measurements had indicated the presence of the DM interaction [8].

The spin–spin interactions, including DM interaction, can be evaluated from the energy-level calculation using an exact diagonalization method [14]. The energy structures in the present systems are described by a magnetic Hamiltonian as follows:

$$H = - \sum_{(ij)} \sum_{\alpha=x,y,z} J_{ij}^{\alpha} \vec{S}_i \cdot \vec{S}_j + \sum_{(ij)} \vec{D}_{ij} [\vec{S}_i \times \vec{S}_j] + \mu_B g \sum_{i=1}^3 \vec{S}_i \cdot \vec{H}_i \quad (6)$$

Here J_{ij}^{α} are the exchange coupling constants between i th and j th spins, in which $J_{1,2}^z \geq J_{2,3}^z \geq J_{3,1}^z$ is defined, \vec{D}_{ij} is the DM vector between i th and j th spins, μ_B is the Bohr magneton, and g factor was determined as $g = 1.959$ by ESR in the similar compound containing the same anionic part [8]. Because it is very difficult to determine the xyz components of the \vec{D}_{ij} , we used the simple

treatment of the DM vectors as a first approximation, which is commonly used in the similar triangle compounds, such as V15 [6,14]. Then, the DM vectors are written as

$$\vec{D}_{1,2} = D_{1,2}^x \hat{x} + D_{1,2}^y \hat{y} + D_{1,2}^z \hat{z}, \quad (7)$$

$$\vec{D}_{2,3} = \frac{1}{2} (-D_{1,2}^x + \sqrt{3} D_{1,2}^y) \hat{x} - \frac{1}{2} (\sqrt{3} D_{1,2}^x \hat{x} + D_{1,2}^y \hat{y}) + D_{1,2}^z \hat{z}, \quad (8)$$

$$\vec{D}_{3,1} = -\frac{1}{2} (D_{1,2}^x + \sqrt{3} D_{1,2}^y) \hat{x} + \frac{1}{2} (\sqrt{3} D_{1,2}^x \hat{x} - D_{1,2}^y \hat{y}) + D_{1,2}^z \hat{z}, \quad (9)$$

$$D = D_{1,2}^x = D_{1,2}^y = D_{1,2}^z = D_{2,3}^z = D_{3,1}^z. \quad (10)$$

In addition, we took into consideration previous ESR results of the similar compound, in which the anisotropy of exchange interactions is $|J_{ij}^z - J_{ij}^x| = 0.24$ K and the zero fields splitting in the $S^T = 3/2$ is the $2\Delta \sim -0.12$ K [8]. Since the positive $J_{ij}^z - J_{ij}^x$ value cannot reproduce the 2Δ in our calculation, we assumed the negative value ($J_{ij}^z - J_{ij}^x = -0.24$ K) for all J_{ij}^z . Here, we calculated the solutions that maximize the $J_{3,1}/J_{1,2}$ ratio, because the slight distortion of the $(VO)_3^{6+}$ triangle would yield only slight deviation of J . Then, the magnetic parameters of $(VO)_3Sb$ are estimated as $J_{1,2}^z = 5.4$ K, $J_{2,3}^z = J_{3,1}^z = 3.5$ K and $D = 1.3$ K, in which δ_1 , δ_2 and 2Δ are well-reproduced. The same values of $J_{2,3}^z$ and $J_{3,1}^z$ originate from the limiting condition of minimizing the $J_{3,1}^z/J_{1,2}^z$ ratio, which is in agreement with the condition of the distortion in $(VO)_3Sb$ (isosceles-triangle-like shape of $(VO)_3^{6+}$ [10]). Here, we noticed that the $J_{3,1}^z/J_{1,2}^z$ ratio is considerably smaller. The small $J_{3,1}^z/J_{1,2}^z$ ratio might result from the distortion of the $(VO)_3^{6+}$ triangle, because the magnitude of J is directly related to the distance between spins. Even in the case of the similar triangle compound ($Na_9[Cu_3Na_3(H_2O)_9(\alpha-AsW_9O_{33})_2] \cdot 26H_2O$) with negligibly small distortion (the difference between the longest and the shortest Cu–Cu distance is only ~ 0.007 Å), the $J_{3,1}^z/J_{1,2}^z$ ratio is less than 1 ($J_{3,1}^z/J_{1,2}^z \sim 0.89$) [6]. In the present compound, the $(VO)_3^{6+}$ triangle is further distorted; the difference between the longest and shortest distance is 0.04 Å [10]. Accordingly, the large difference of J_{ij} values ($J_{3,1}^z/J_{1,2}^z \sim 0.65$) might agree with the larger distortion of $(VO)_3^{6+}$ triangle. On the other hand, the value of D amounting to 24% of $J_{1,2}^z$ is slightly larger than the typical value of the magnitude for these systems [6]. The DM interaction is derived by extending the theory of superexchange interaction with the effect of spin–orbit coupling [15]. Since the V^{4+} ions of the present system are surrounded by five oxygen ions, which might lead to many DM interaction pathways, the molecular structure seems to lead to the relatively large value of D .

In the case of $(VO)_3Bi$, the magnetic parameters cannot be estimated in the same way, because the 2Δ and the anisotropy of J_{ij}^z are not known. Therefore, we assumed that the DM interaction amounts to 24% of $J_{1,2}$ and that the anisotropy is negligible. Then, the magnetic parameters are obtained as $J_{1,2} = 4.1$ K, $J_{2,3} = J_{3,1} = 2.7$ K and $D = 1.0$ K. Since the distortion in $(VO)_3Bi$ has been reported to be of the same magnitude as that of $(VO)_3Sb$ by X-ray measurements [8,10], the values obtained for the magnetic parameters of $(VO)_3Bi$ seem to be reasonable.

Finally, we show the calculated energy level diagrams of $(VO)_3Sb$ for two arrangements of the $H \parallel z$ and the $H \parallel x$ in Fig. 8. The energy level diagrams clearly show the angular dependence of the magnetic fields, which is usually reported in the calculation containing the DM interaction [6,12]. Around 5.5 T, the magnetic field dependence of the energy gap between the lowest energy state and the first excited state is significantly small as a result of

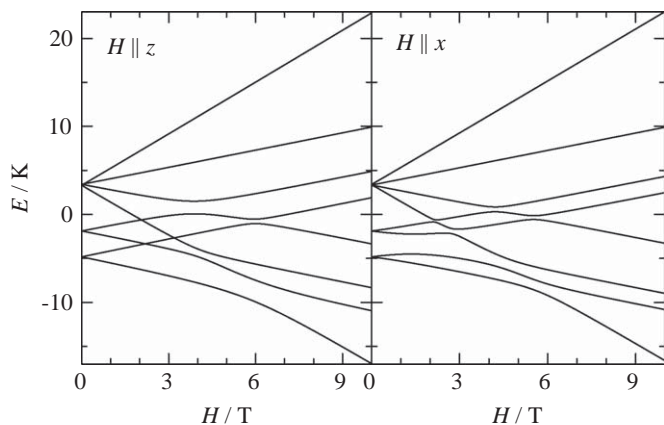


Fig. 8. Energy level diagrams of $K_{12}[(VO)_3(SbW_9O_{33})_2] \cdot 15H_2O$. The values of the spin–spin interactions are given in the text. Left: applied magnetic field H parallel to the z axis. Right: applied magnetic field H along the x axis.

the DM interaction. Although the quantitative agreement between the observed and calculated heat capacity under a magnetic field is not adequate, presumably because of the random orientation of the magnetic fields in the heat capacity measurements, the energy-level repulsion can qualitatively explain the small magnetic field dependence of the heat capacity, which is evidence of a large DM interaction in the present compound.

4. Conclusion

We have measured the low-temperature heat capacity of two molecular clusters, $K_{12}[(VO)_3(SbW_9O_{33})_2] \cdot 15H_2O$ and $K_{12}[(VO)_3(BiW_9O_{33})_2] \cdot 29H_2O$. The broad anomalies caused by the magnetic fields are observed in both compounds, and are analyzed in terms of the energy-level splitting under the influence of magnetic fields. The analysis of entropy and the fit of heat capacity reveal that the ground state is a doublet, in which the energy gap between ground and the first excited doublets are 2.9 and 2.3 K for $K_{12}[(VO)_3(SbW_9O_{33})_2] \cdot 15H_2O$ and $K_{12}[(VO)_3(BiW_9O_{33})_2] \cdot 29H_2O$, respectively. In addition, the heat capacity near 5.5 T shows the small magnetic field dependence, suggesting the existence of DM interaction. We carried out a numerical calculation to estimate the spin–spin interactions, including the DM interaction, and pro-

duced an energy level diagram showing a small magnetic field dependence at about 5.5 T.

Acknowledgments

This work was supported by a Grant-in-Aid JSPS (Grant no. 19.9728). We would like to thank Rie Otake for the help during experiment.

References

- [1] L. Thomas, F. Lioni, R. Ballou, D. Gatteschi, R. Sessoli, B. Barbara, *Nature* (London) 383 (1996) 145–147.
- [2] F. Luis, F.L. Mettes, J. Tejada, D. Gatteschi, L.J. de Jongh, *Phys. Rev. Lett.* 85 (2000) 4377–4380.
- [3] D. Gatteschi, A. Caneschi, L. Pardi, R. Sessoli, *Science* 265 (1994) 1054–1058.
- [4] W. Wernsdorfer, R. Sessoli, *Science* 284 (1999) 133–135.
- [5] C. Raghun, I. Rudra, S. Ramasesha, D. Sen, *Phys. Rev. B* 62 (2000) 9484–9492.
- [6] K.Y. Choi, Y.H. Matsuda, H. Nojiri, U. Kortz, F. Hussain, A.C. Stowe, C. Ramsey, N.S. Dalal, *Phys. Rev. Lett.* 96 (2006) 107202.
- [7] I. Chiorescu, W. Wernsdorfer, A. Müller, S. Miyashita, B. Barbara, *Phys. Rev. B* 67 (2003) 020402(R).
- [8] T. Yamase, E. Ishikawa, K. Fukaya, H. Nojiri, T. Taniguchi, T. Atake, *Inorg. Chem.* 43 (2004) 8150–8157.
- [9] T. Yamase, B. Botar, E. Ishikawa, K. Fukaya, *Chem. Lett.* (2001) 56–57.
- [10] $K_{12}[(VO)_3(SbW_9O_{33})_2] \cdot 15H_2O$ was synthesized by the same procedure used for synthesizing $K_{11}H[(VO)_3(SbW_9O_{33})_2] \cdot 27H_2O$ [9]. Although the composition was slightly different from $K_{11}H[(VO)_3(SbW_9O_{33})_2] \cdot 27H_2O$, the anionic part including $(VO)_3$ plane was little changed. Thus, the magnetic property of $K_{12}[(VO)_3(SbW_9O_{33})_2] \cdot 15H_2O$ should be similar to that of $K_{11}H[(VO)_3(SbW_9O_{33})_2] \cdot 27H_2O$. X-ray diffraction data of $K_{12}[(VO)_3(SbW_9O_{33})_2] \cdot 15H_2O$ was collected on a Rigaku-RAXIS-RAPID imaging-plate diffractometer employing the monochromatized $MoK\alpha$ radiation ($\lambda = 0.71069 \text{ \AA}$) at 23 °C. The structure was solved by direct methods (MULTAN 88) and refined using a full-matrix least-squares refinement procedure. Crystal data: molecular weight = 554 883, monoclinic, space group $P21/m$ (No. 11), $a = 12.949(8)$, $b = 18.18(8)$, $c = 17.67(1)$, $\alpha = 90$, $\beta = 107.51(4)$, $\gamma = 90$, $V = 3965(5) \text{ \AA}^3$, $Z = 2$, $D = 4.647 \text{ g cm}^{-3}$, $\mu = 277.672 \text{ cm}^{-1}$. The distances between V^{4+} ions are 5.32, 5.36 and 5.36 Å in $K_{12}[(VO)_3(SbW_9O_{33})_2] \cdot 15H_2O$, while they are 5.411, 5.453 and 5.464 Å in $K_{11}H[(VO)_3(SbW_9O_{33})_2] \cdot 27H_2O$. Some of the K atoms and solvent water O atoms were disordered in $K_{12}[(VO)_3(SbW_9O_{33})_2] \cdot 15H_2O$: the occupancies of K7–K8 and O48–O50 were fixed at 1/2 throughout the refinement.
- [11] K. Kambe, *J. Phys. Soc. Jpn.* 5 (1950) 48–51.
- [12] H. De Raedt, S. Miyashita, K. Michielsen, M. Machida, *Phys. Rev. B* 70 (2004) 064401.
- [13] Y. Kohama, T. Tojo, H. Kawaji, T. Atake, S. Matsuishi, H. Hosono, *Chem. Phys. Lett.* 421 (2006) 558–561.
- [14] Y. Shapira, V. Bindilatti, *J. Appl. Phys.* 92 (2002) 4155–4185.
- [15] T. Moriya, *Phys. Rev.* 120 (1960) 91–98.